Simona Silvia Merola, Paolo Sementa, Cinzia Tornatore
Istituto Motori – CNR, Napoli (Italy)

In-cylinder formation and exhaust emission of particulates from a 4-stroke engine of a 2-wheel vehicle

The efficiency of small engines in two-wheel vehicles can be further improved especially at low speeds and high loads. In these conditions fuel consumption and pollutant emission should be reduced maintaining the performance levels. This optimization can be realized only by the improvement in the basic knowledge of the thermo-fluid dynamic phenomena occurring during the combustion process. It is known that during the fuel injection phase in PFI SI engines, thin films of liquid fuel can form on the valves surface and on the cylinder walls. Successively the fuel films interact with the intake manifold and the combustion chamber gas flow. During the normal combustion process, it is possible to achieve gas temperature and mixture strength conditions that lead to fuel film ignition. This phenomenon can create diffusion-controlled flames. These flames persist well after the normal combustion event and induce the formation and then the exhaust emission of soot and unburned hydrocarbons. In this paper, experimental activities were carried out in the combustion chamber of a single-cylinder optical engine in order to investigate the in-cylinder formation and exhaust emission of particulates from a 4-stroke engine of a 2-wheel vehicle. The engine was equipped with the four-valve head of a commercial scooter engine and it was fuelled with European commercial gasoline. Cycle-resolved digital imaging and high spatial resolution visualization with two-color pirometry tool were used to follow in detail the flame front propagation and related phenomena. In particular the inception of diffusion-controlled flames near the valves and on the cylinder walls was studied. These flames induced the in-cylinder formation of unburned hydrocarbons and soot particles and the following exhaust emissions. The optical data were correlated with conventional combustion pressure measurements and particulate exhaust emission. The effect of three-way catalyst was investigated too.

Tworzenie i emisja cząstek stałych w wydechu silnika czterosuwowego pojazdów dwukołowych

Sprawność małych silników pojazdów dwukołowych można poprawić, szczególnie przy dużych obciążeniach i niskich prędkościach. W tych warunkach dla utrzymania odpowiedniego poziomu pracy emisja zanieczyszczeń i zużycie paliwa powinny zostać obniżone. Taką optymalizację można było przeprowadzić tylko na podstawie wiedzy o dynamice zjawisk przepływu ciepła zachodzących podczas procesu spalania. Wiadomo jest, że w fazie wtrysku paliwa do silnika typu PFI (port-fuel-injected) z zapłonem iskrowym (SI), na powierzchni zaworów i ścianach cylindra mogą tworzyć się cienkie warstewki ciekłego paliwa. Z kolei warstewki paliwa oddziałują z przepływem gazów w kolektorze i komorze spalania. W trakcie normalnego procesu spalania możliwe jest osiągnięcie temperatury gazu i mieszanki umożliwiającej zapłon filmu paliwa. To zjawisko może prowadzić do wytwarzania płomieni sterowanych dyfuzyjnie. Takie, utrzymujące się dłuższy czas po normalnym spaleniu mieszanki, płomienie mogą być w dalszym ciągu przyczyną tworzenia i emisji sadzy oraz niespalonych węglowodorów. W pracy opisano badania doświadczalne nad tworzeniem i emisją cząsteczek stałych (PM), prowadzone metodą optyczną w komorze silnika jednocylindrowego, czterosuwowego, przeznaczonego dla pojazdów dwukołowych. Silnik został wyposażony w głowicę czterozaworową z handlowego skutera i był zasilany handlową benzyną europejską. Do dokładnej, cyfrowej analizy obrazu wykorzystano narzędzia trójwymiarowej pirometrii dwubarwnej o wysokiej rozdzielczości, przede wszystkim dla szczegółowego zbadania propagacji frontu płomienia i zachodzących przy tym zjawisk. Głównie badano powstawanie płomieni sterowanych dyfuzyjnie w pobliżu zaworów i na ściankach cylindra. Te płomienie powodują tworzenie się w cylindrze cząsteczek sadzy i pozostawanie niespalonych węglowodorów, obserwowanych następnie w wydechu. Uzyskane dane z pomiarów optycznych skorelowano z konwencjonalnymi pomiarami ciśnienia i emisji cząstek. Badano również efektywność katalizatora trójdrożnego.

Introduction

Motorcycles and scooters are very popular in most of Asian and in many European countries. The number of these vehicles is expanding rapidly because they allow a high mobility in the congested areas at lower costs than small automobiles. On the other hand, 2-wheel vehicles are significant sources of hydrocarbons (HCs), carbon monoxide (CO), and particulate matter (PM). To reduce their negative environmental impact, many countries have implemented some pollution control programs [1, 2, 3, 4]. The current emission standard Euro-3 has led to the implementation of catalyst systems, which are not low cost devices. Thus low cost solutions for the pollutant emission reduction are required. In particular a strong optimization of engine efficiency at low speeds and high loads is necessary.

This target can be reached only by the improvement in the basic knowledge of the thermo-fluid dynamic phenomena occurring during the injection and the combustion process.

In this work the in-cylinder formation and exhaust emission of particulates due to the burning of the thin films of liquid fuel on the valves surface and on the cylinder walls was investigated [5, 6]. The phenomenon is induced by interaction between the fuel deposited in the combustion chamber with the normal combustion flame front. This interaction induces the fuel film ignition and then the inception of strong diffusion-controlled flames. The flames persist well until the opening of exhaust valves and they induce the formation of unburned hydrocarbons, carbonaceous compounds and soot [7, 8].

A single cylinder engine constituted by an elongated optical accessible piston and equipped with the head and injection system of a reference real engine was used. Cycle resolved digital imaging was applied to follow the flame propagation from the spark ignition to the exhaust phase. High spatial resolution visualization with two-color pirometry tool was used to detect the in-cylinder particulates and soot distribution. The optical results were correlated with the engine parameters and with the exhaust emissions measured by conventional methods.

Experimental apparatus

Transparent engine

The experiments were performed in an optically accessible single-cylinder, Port Fuel Injection (PFI), Spark Ignition (SI) four-stroke engine (Fig. 1). The engine bore and stroke are 72 mm, 60 mm and the geometric compression ratio was 11. The engine was equipped with the cylinder head of a commercial 250 cc motorcycles engine with the same geometrical specifications (bore, stroke, compression ratio) of the research engine. The head had four valves and a centrally located spark plug. The injection system was the same as that mounted on the reference real engine. The experimental engine reached 7.9 kW and 14.7 Nm at the maximum speed of 5000 rpm.

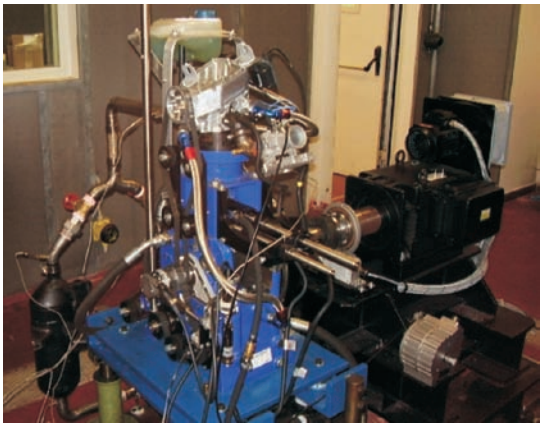

Fig. 1. PFI – SI optical accessible engine used for the experiments

Rys. 1. Stosowany w badaniach silnik z zapłonem iskrowym typu PFI wyposażony w akcesoria optyczne

A quartz pressure transducer was flush-installed in the combustion chamber to measure the combustion pressure. The in-cylinder pressure, the rate of chemical energy release and all related parameters were evaluated on an individual cycle basis and/or averaged across 400 cycles [9].

A section of the concentric flat-bottomed piston bowl was replaced with a sapphire window to enable the passage of optical signals coming from the combustion chamber. To reduce the window contamination by lubricating oil, the elongated piston arrangement was used together with self-lubricating Teflon-bronze composite piston rings in the optical section.

Setup for optical measurements

Figure 2 shows the experimental apparatus for optical investigations. During the combustion process, the light passed through the sapphire window and it was reflected toward the optical detection assembly by a 45° inclined UV-visible mirror located in the bottom of the engine.

The cycle resolved digital imaging was performed by 8-bit high speed camera (512 × 512 pixel) equipped with a 50 mm focal Nikon lens. The spectral range of the high speed camera extended from 390 nm to 900 nm. A camera region of interest was selected (360 × 360 pixel) to obtain the best match between spatial and temporal resolution. This optical assessment allowed a spatial resolution around 0.25 mm/pixel and a frame rate of 7188 fps. The exposure time was fixed at 10 μs.

In this work, two locations were selected in the combustion chamber to follow the evolution of the local luminous signal on the intake valve (loc. 1) and on the exhaust valve (loc. 2). Each location had an area of 3 × 3 pixel.

A post-processing of the optical data was realized by means of Labview™ of National Instruments to convert each frame of a camera sequence into an 8-bit image and then into 360 × 360 numerical matrix. In this way the

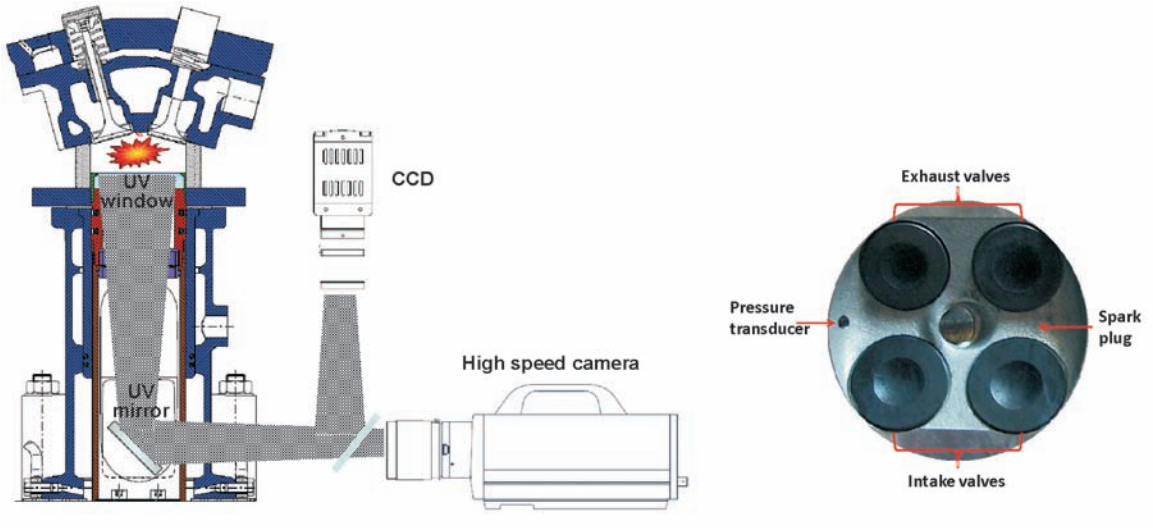

Fig. 2. Sketch (a) of the experimental setup for the cycle resolved digital imaging and (b) of the bottom field of view of the combustion chamber

Rys. 2. Schemat (a) układu doświadczalnego rozwiązującego cykl digitalizacji obrazu oraz (b) widok z dołu komory spalania. UV Window – okno przepuszczalne dla nadfioletu, UV mirror – zwierciadło nadfioletu, CCD – charge-coupled device – rejestrator analogowy, High speed camera – kamera o dużej prędkości, Exhaust valves – zawory wydechowe, Intake valves – zawory dolotowe, Pressure transducer – przetwornik ciśnienia, Spark plug – świeca zapłonowa

temporal evolution of the local luminosity from each location of the combustion chamber and the integral one was evaluated for each combustion cycle.

Moreover, fixing a threshold of 2^6 on 2^8 counts for the pixel luminosity, flame area and outline were obtained. Thus the distance of each pixel in the flame outline from the centre of the combustion chamber was calculated. The flame radius was obtained by the average of all these distances [10, 11].

2D soot flame visualization was obtained by a 12-bit digital CCD color camera coupled with a 50 mm focal length f/3.8 Nikon lens. The CCD had a 640 × 480 pixel matrix with a pixel size of 9.9 × 9.9 μm^2. This optical assessment allowed a spatial resolution around 0.1 mm/pixel. The spectral range of the camera was 290-800 nm. Spatial distribution of soot temperature and concentration was obtained by two color method. The soot-emission wavelengths were selected by edge filters. More details about this methodology are reported in [12]. The camera was not a cycle resolved detector and each image was detected at a fixed crank angle of different engine cycles. Both the cameras (CMOS and CCD) and the engine were synchronized by sending the Crank Angle Encoder signal through a unit delay. AVL Indimodul recorded the TTL signal from the camera acquisitions together with the signal acquired by the pressure transducer. In this way, it was possible to determine the crank angles where optical data were detected.

Exhaust measurements

Steady-state measurements of CO, CO_2, O_2, HC and NO_x were performed in the raw exhaust by commercial analysers. CO, CO_2 and HC were measured by Non-Dispersive Infrared Detectors (NDIR); NO_x and O_2 were detected through electrochemical sensor. An opacimeter was used to evaluate the particulate mass concentration [13].

Results and discussion

Engine operating conditions

All of the experimental investigations were carried out at an engine speed of 3000 rpm at wide open throttle. The intake air temperature was fixed at 298 K and the cooling water temperature was set at 333 K. Commercial gasoline with octane number 95 was used. For all the test cases, the fuel injection occurred at 300 CAD BTDC at 3 bar. Moreover, the injection duration was fixed in order to reach the same equivalence ratio of the commercial reference engine in the same operative conditions. The lambda value was measured by an oxygen sensor at the engine exhaust. The

Table 1. Engine operating conditions
Tablica 1. Warunki testu silnikowego

Test #	TWC	Lambda	COV_{lambda} [%]	IMEP [bar]	COV_{IMEP} [%]	BSFC [g/kWh]
1	without	0.9	2.6	6.9	0.9	555.3
2	with	0.9	2.5	7.0	1.0	563.0

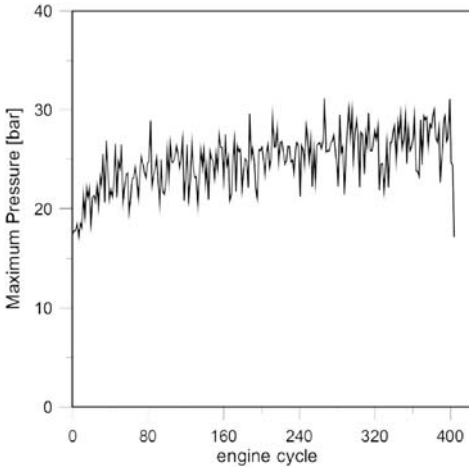

Fig. 3. Time evolution on 400 consecutive engine cycles of the maximum pressure signal measured in the combustion chamber for the condition 1

Rys. 3. Zmiany zachodzące w czasie przy 400 kolejnych cyklach pracy silnika dla pomiaru sygnału maksymalnego ciśnienia w komorze spalania, w warunkach 1

spark timing was always fixed to operate at the maximum brake torque (22 CAD BTDC). Tests with and without TWC were performed. In the selected engine conditions the exhaust temperature was lower than catalyst activation temperature. Moreover, the exhaust temperature was maintained constant using thermo-control device placed upstream TWC.

IMEP and COV (Table 1) were comparable with the typical ones of the commercial reference engine. The thermal evolution and fluctuation of the maximum pressure signal due to the cyclic variation resulted satisfactory, as shown in Figure 3. This result demonstrated that the heat transfer between the different components of the optical engine could be considered as negligible.

The pressure measurements and the exhaust data give real-time cycle-resolved overall information on the combustion process but they don't allow a local analysis. The optical techniques are a powerful tool for detailing the thermal and fluid dynamic phenomena that occur in the combustion chamber. On the other hand, optical methodologies need high-costs specific engines and instrumentations.

In this work, cycle resolved imaging and high spatial resolution visualization of the combustion process were performed.

Figure 4 reports the typical cycle resolved flame propagation detected in the combustion chamber for the selected condition 1 and the corresponding pressure trace. The crank angles where the acquisition was performed are highlighted with dots.

For all the both selected test cases, the first evidence of the flame inception occurred around 2 CAD after the spark ignition. Then the flame front moved from the centrally located spark plug with a radial-like behavior for about 20-25 CAD. When the flame reached the intake valves region, an asymmetry in the flame front shape was observed. In fact, the flame reached first the cylinder walls in the exhaust valves region.

This phenomenon was due to the fuel film deposited on the intake valves. During the injection process the fuel drips on the intake valves steams, then it accumulates on the valves seats. This deposit is drawn by the gravity onto the valve head where it remains as film due to the surface tension. Once formed in the combustion chamber, the fuel film develops dynamically under the effect of the gas flow influencing the composition of the mixture and hence the combustion process [14, 15, 16, 17]. In fact, the flame propagation is influenced by the thermodynamic conditions, the mixture composition and the local turbulence intensity. When a flame propagates in the normal direction to a region with equivalence ratio gradient, each part of the front evolves in a field with varying fuel concentration. This induces variation of the propagation speed along the flame front and an increase in flame wrinkling.

It should be outlined that several bright spots were detected in the burned gas before the flame front reached the chamber walls. The bright spots were due to the fuel deposits on the optical window caused by the strip atomization of the fuel squeezing. The fuel deposits created fuel-rich zones with sub-millimeter size that ignited when reached by the normal flame front. When the injection occurred in the open valves condition, this effect was enhanced by the partial carrying of the injected fuel droplets directly into the combustion chamber due to the gas flow. An amount of these droplets stuck on the cylinder walls and a part was deposited on the piston surface.

The presence of the fuel deposits as squeezed film or impinged droplets had direct effect on the flame radius evolution in terms of kernel cyclic variability and flame stability [18, 19]. Figure 5 reports the trend of the flame radius evaluated on 400 consecutive cycles. It must be noted that around 5 CAD ATDC a change in flame radius evolution was detected. This was due to the approaching

to the intake valve region. The higher fuel amount near the intake valves induced fuel-richer zones that slowed down the flame front. After the interaction with the intake valves, the flame occupied the whole optical field of view of the combustion chamber around 15 CAD ATDC.

As already observable in Figure 4, when the flame front interacted with the fuel deposits on the intake valves, diffusion-controlled flames with high luminosity were observed [14-17]. These flames persisted in the late combustion phase and their optical evidence could be detected until the exhaust valves opening (25% open @150 CAD ATDC). The formation of diffusive flames was possible since the oxygen was not completely consumed after the normal flame front propagation.

The spatial distribution of diffusion-controlled flames can be analyzed through the image selection reported in Figure 6. It shows the flame emissions revealed just after the crank angle of maximum pressure until the end of the combustion process. The highly intense flames were observed especially near the intake valves, as expected.

Figure 7 reports the flame luminosity averaged on the chamber volume and measured in the two selected locations. It can be noted that the luminosity of the diffusion controlled flames is still high

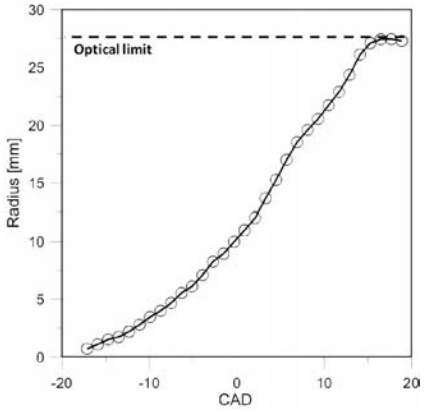

Fig. 5. Time evolution of the mean flame radius evaluated on 400 consecutive cycles

Rys. 5. Czas przyrostu średniego promienia płomienia podczas 400 kolejnych cykli

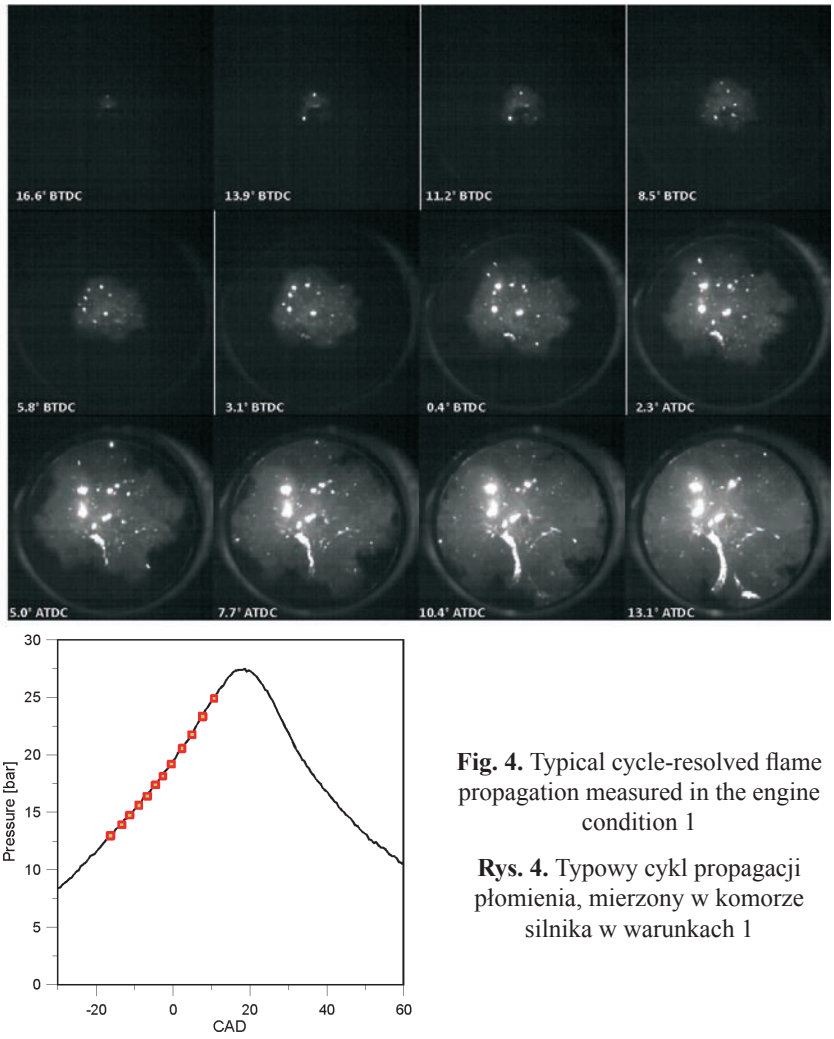

Fig. 4. Typical cycle-resolved flame propagation measured in the engine condition 1

Rys. 4. Typowy cykl propagacji płomienia, mierzony w komorze silnika w warunkach 1

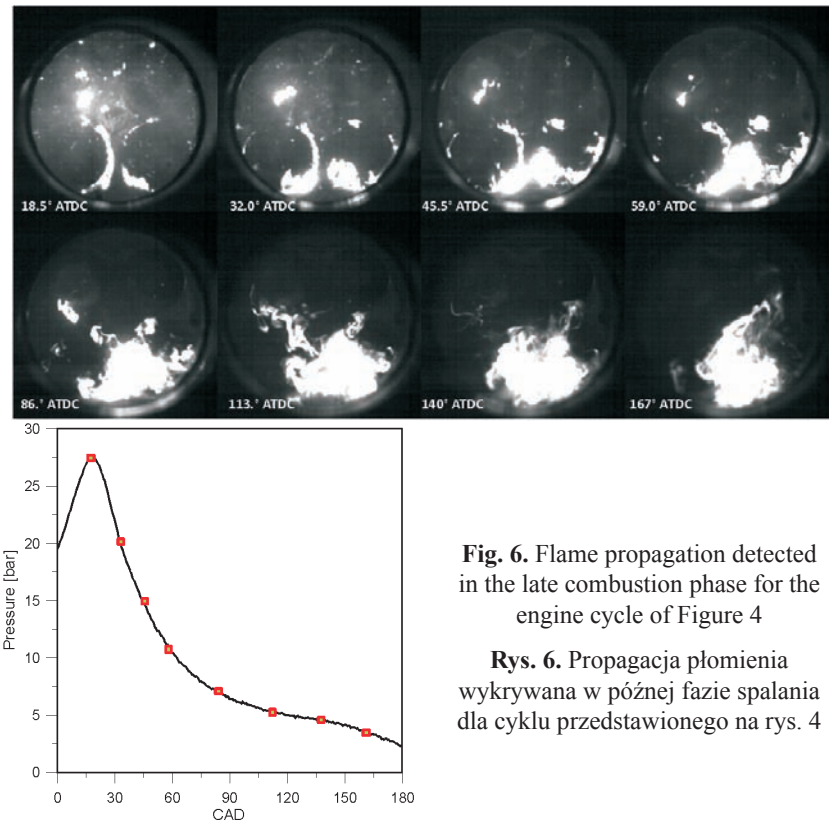

Fig. 6. Flame propagation detected in the late combustion phase for the engine cycle of Figure 4

Rys. 6. Propagacja płomienia wykrywana w późnej fazie spalania dla cyklu przedstawionego na rys. 4

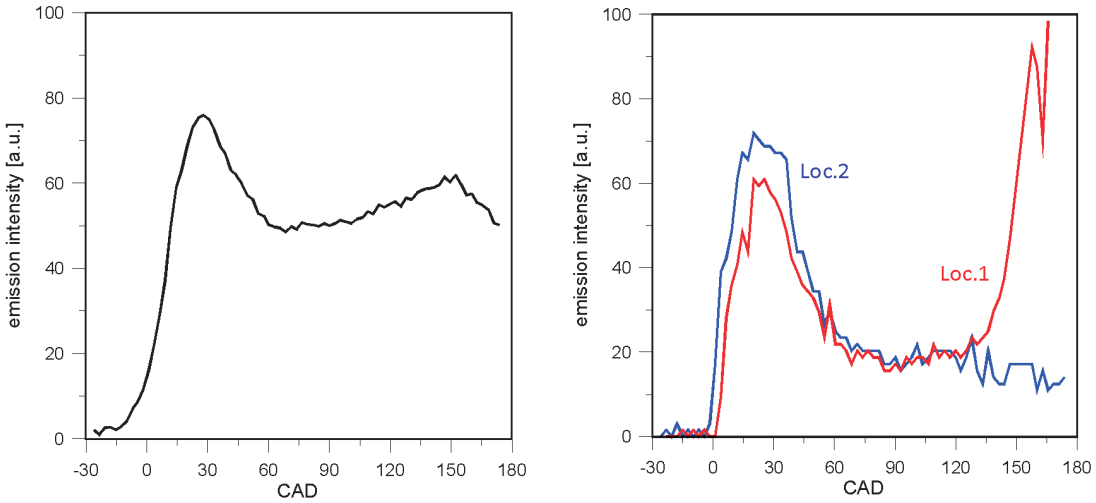

Fig. 7. Flame emission luminosity (a) averaged on the combustion chamber volume and (b) detected in the two selected locations of the combustion chamber

Rys. 7. Jasność płomienia (a) uśredniona w objętości komory spalania oraz (b) wykrywana w dwóch wybranych lokalizacjach w komorze spalania

at the exhaust valves opening (Figure 7a). The luminous intensity and its rate in the exhaust valve region were higher than the intake valve one (Figure 7b). This was due to the distortion of the flame front caused by the fuel film deposits on the intake valves. Around 20 CAD ATDC the integral intensity reached the maximum value that coincided with the highest combustion pressure and heat release. Then the combustion intensity decreased but a new increase in luminosity was detected. This was due to the fuel deposits burning in the intake valves region. This phenomenon did not contribute to the engine work and it did not influence the pressure signal [20, 21].

Previous spectroscopic investigations showed that the diffusion-controlled flames spectra are characterized by a strong continuous contribution that increases with the wavelength in the visible range, typical of soot material [22, 23]. In order to study this effect, optical system for high spatial resolution visualization was used. The system was also equipped with hardware for the evaluation of soot spatial distribution by means of two-color pirometry technique. Figure 8 reports the typical sequence of flame emission images and soot distribution ones.

As it can be observed in the results obtained by two-color pirometry technique, the soot was mainly formed in the intake valves region. The principal source of soot was the diffusion-controlled flame generated by the fuel deposits on the intake valves.

Figure 9 reports the time evolution of the integral soot measured in the combustion chamber. Two different phases

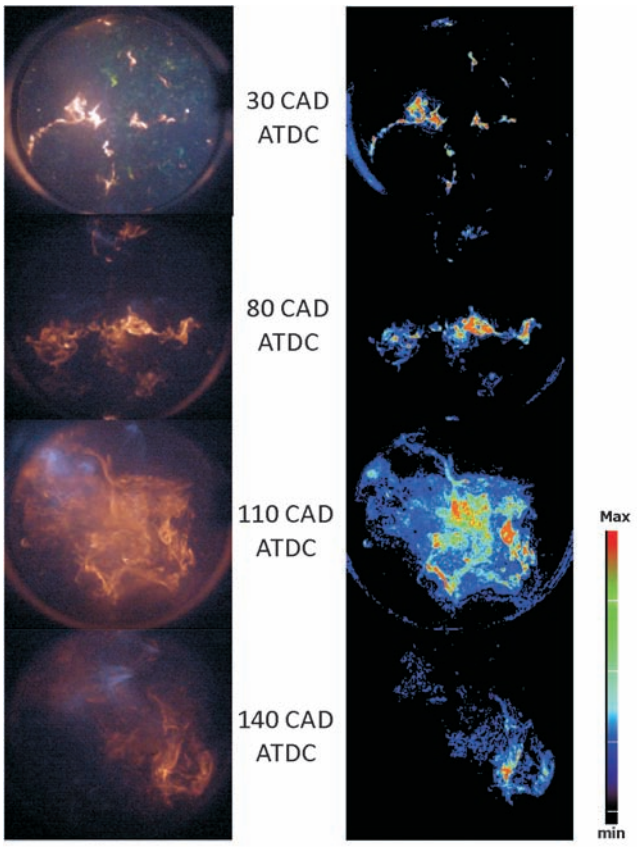

Fig. 8. High spatial resolution (a) flame emission and (b) soot spatial distribution detected in the combustion chamber

Rys. 8. Wysoka rozdzielczość przestrzenna (a) emisja płomienia oraz (b) przestrzenna dystrybucja sadzy, obserwowane w komorze spalania

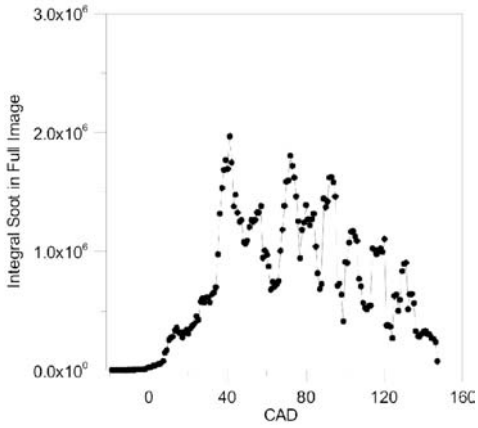

Fig. 9. Integral soot measured in the combution chamber

Rys. 9. Całkowite pomiary sadzy w komorze spalania

could be distinguished. In the first one, until 40 CAD, the soot formation mechanism was favored and the soot concentration increased. In the second one, a decrease in soot concentration could be observed, this was due to the soot oxidation predominance on the soot formation. Anyway, the soot reduction rate at the exhaust valves opening was not sufficient to oxidize all the particulate.

In conclusion, diffusion-controlled flame emission can be correlated to the particulate emission at the exhaust. In order to better understand the effect of the TWC on the particulate emission, the exhaust opacity with and without catalyst was measured. It is known that the opacimeter measurements suffer the interference of gaseous species as NO_2 and high-mass HC. Nevertheless, in low temperature condition the effect of the TWC on gas emission was negligible, thus the relative variation of opacity was due to the particulate reduction. In the selected engine operating condition, the TWC induced an opacity reduction at low temperature around 20%. This result was due to the inertial impaction on the catalyst channel faces. The TWC worked as a sort of particulate filter [24]. It was demonstrated by the temporal evolution of opacity downstream TWC realized on 6 tests and reported in Figure 10.

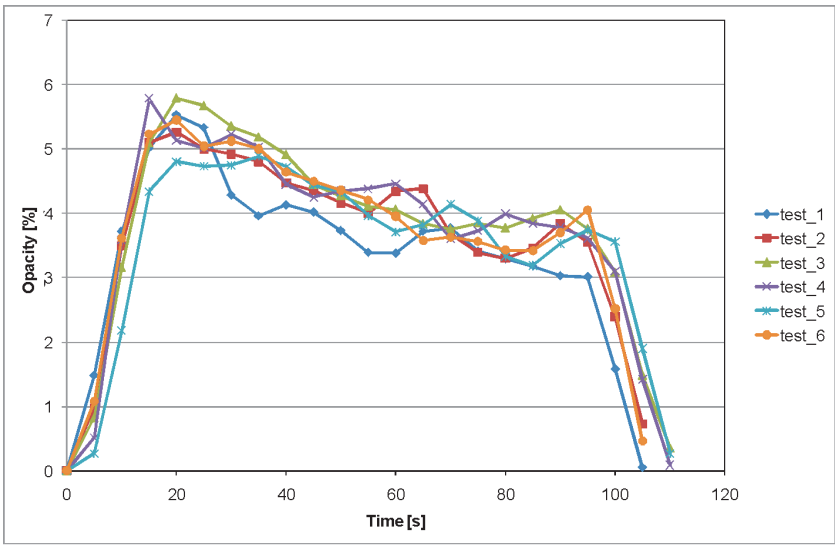

Fig. 10. Temporal evolution of opacity downstream TWC

Rys. 10. Zmiany zaciemnienia strumienia gazów (katalizator trójdrożny) w czasie

Conclusions

Cycle-resolved digital imaging, high spatial resolution visualization and two-color pyrometry were applied to characterize the flame propagation in the combustion chamber of a single-cylinder 4-stroke optical engine equipped with the 4-valve head of a commercial scooter engine. All of the experimental investigations were carried out at 3000 rpm in the same operative conditions of the commercial reference engine. In the selected engine conditions the exhaust temperature was lower than catalyst activation temperature.

For all the selected engine conditions, the flame front spread from the spark plug with radial-like behavior until it reached the intake valves region. Then an asymmetry in the flame front shape was observed. This was due to the fuel film deposits formed during the injection process by the fuel dripping and accumulation on the intake valves steams and seats. As a consequence, intense diffusion-controlled flames were observed especially near the intake valves until the opening of the exhaust valves. These flames persist well after the normal combustion event and induce the formation and then the exhaust emission of soot and unburned hydrocarbons. These results were confirmed by high spatial resolution digital imaging and two color pirometry that was employed to measure the in-cylinder soot concentrations.

In-cylinder optical investigations were correlated with the engine parameters and exhaust emissions measured by conventional methods. In particular, in the low temperature

condition the TWC induced a well measurable opacity reduction. Thus TWC worked as a particulate filter and decreased the number of large solid particles due to the inertial impaction on the catalyst channel faces.

Recenzent: doc. dr Michał Krasodomski

Acknowledgements

The authors are grateful to Mr. Carlo Rossi and Mr. Bruno Sgammato for the assessment of the optical engine and for the support in the experimental activities.

References

[1] Han X., Naeher L.P.: *A review of traffic-related air pollution exposure assessment studies in the developing world.* Environmental International 32, 106-120, 2006.

[2] Singh S.K.: *Future mobility in India: implications for energy demand and CO_2 emission*. Transport Policy 13, 398-412, 2006.

[3] Vasic A.M., Weilenmann, M.: *Comparison of real-world emissions from two wheelers and passenger cars*. Environmental Science and Technology 40, 149-154, 2006.

[4] Ntziachristos L., Mamakos A., Samaras Z., Xanthopoulos A., Iakovou, E.: *Emission control options for power two wheelers in Europe*. Atmospheric Environment 40, 4547-4561, 2006.

[5] Shin Y., Cheng W.K., Heywood J.B.: *Liquid Gasoline Behaviour in the Engine Cylinder of a SI Engine*. SAE Paper n. 941872, 1994.

[6] Zhu G.S., Reitz R.D., Xin J., Takabayashi,T.: *Modelling Characteristics of Gasoline Wall Films in the Intake Port of Port Fuel Injection Engines*. Int. J. of Engine Research, vol. 2, N. 4, 231-248, 2001.

[7] Bockhorn H. (Ed.): *Soot Formation in Combustion: Mechanisms and Models*. Springer, Berlin, 1994.

[8] Drake M.C., Fansler T.D., Solomon A.S. and Szekely G.A. Jr.: *Piston fuel films as a source of smoke and hydrocarbon emissions from a wall-controlled spark-ignited direct-injection engine*. SAE Paper No. 2003-01-0547, 2003.

[9] Heywood J.B.: *Internal Combustion Engine Fundamentals*. New York: McGraw-Hill, 1988.

[10] Hacohen J., Belmont M.R., Thurley R.W.F., Thomas J.C., Morris E.L.: *Buckingham DJ. Experimental and Theoretical Analysis of Flame Development and Misfire Phenomena in a Spark-ignition Engine*. SAE paper n. 920412, 1992.

[11] Merola S.S., Vaglieco B.M., Formisano G., Lucignano G., Mastrangelo G.: *Flame Diagnostics in the Combustion Chamber of Boosted PFI SI Engine*. SAE paper n. 2007-24-0003, 2007.

[12] AVL user manual, AVL Graz, Austria 2003.

[13] Mörsch O., Sorsche P., (DaimlerChrysler AG): *Investigation of Alternative Methods to Determine Particulate Mass Emission*s, http://www.oica.net/htdocs.

[14] Costanzo V.S., Heywood J.B.: *Mixture Preparation Mechanisms in a Port Fuel Injected Engine*. SAE Paper No. 2005-01-2080, 2005.

[15] Gold M.R., Arcoumanis C., Whitelaw J.H., Gaade J., Wallace, S.: *Mixture Preparation Strategies in an Optical Four-Valve Port-Injected Gasoline Engine*. Int. J. of Engine Research, vol. 1, N. 1, 41-56, 2000.

[16] Nogi T., Ohyama Y., Yamauchi T. and Kuroiwa H.: *Mixture Formation of Fuel Injection Systems in Gasoline Engines*. SAE Paper n. 880558, 1988.

[17] Meyer R., Heywood J.B.: *Liquid Fuel Transport Mechanisms into the Cylinder of a Firing Port-Injected SI Engine During Start Up*, SAE Paper No. 970865, 1997.

[18] Bianco Y., Cheng W., Heywood, J.: *The Effects of Initial Flame Kernel conditions on Flame Development in SI Engines*. SAE paper n. 912402, 1992.

[19] Witze P., Hall M., Bennet M.: *Cycle-resolved Measurements of Flame Kernel Growth and Motion Correlated with Combustion Duration.* SAE paper n. 900023, 1990.

[20] Nogi T., Ohyama Y., Yamauchi, T. and Kuroiwa H.: *Mixture Formation of Fuel Injection Systems in Gasoline Engines*. SAE Paper n. 880558, 1988.

[21] Witze P.O. and Green, R.M.: *LIF and Flame-Emission Imaging of Liquid Fuel Films and Pool Fires in an SI Engine During a Simulated Cold Start*. SAE Paper n. 970866, 1997.

[22] Merola S.S., Sementa, P., Tornatore C. and Vaglieco B.M.: *Effect of Injection Phasing on Valves and Chamber Fuel Deposition Burning in a PFI Boosted Spark-Ignition Engine*. SAE Paper n. 2008-01-0428, 2008.

[23] Merola S.S., Sementa P., Tornatore C., Vaglieco B.M.: *Effect of the Fuel Injection Strategy on the Combustion Process in a PFI Boosted Spark-Ignition Engine*. Proc. ECOS 2008 Conference, Volume I, Page 467, 2008.

[24] Abdul-Khalek I.S., Kittelson D.B.: *Real time measurement of volatile and solid exhaust particles using a catalytic stripper*. SAE Paper No. 950236, 1995.